Cells activated for wound repair have the potential to direct collective invasion of an epithelium

Brigid M. Bleaken, A. Sue Menko*, and Janice L. Walker*
Department of Pathology, Anatomy and Cell Biology, Thomas Jefferson University, Philadelphia, PA 19107

ABSTRACT **Mechanisms regulating how groups of cells are signaled to move collectively from their original site and invade surrounding matrix are poorly understood. Here we develop a clinically relevant ex vivo injury invasion model to determine whether cells involved in directing wound healing have invasive function and whether they can act as leader cells to direct movement of a wounded epithelium through a three-dimensional (3D) extracellular matrix (ECM) environment. Similar to cancer invasion, we found that the injured cells invade into the ECM as cords, involving heterotypical cell–cell interactions. Mesenchymal cells with properties of activated repair cells that typically locate to a wound edge are present in leader positions at the front of ZO-1–rich invading cords of cells, where they extend vimentin intermediate filament–enriched protrusions into the 3D ECM. Injury-induced invasion depends on both vimentin cytoskeletal function and MMP-2/9 matrix remodeling, because inhibiting either of these suppressed invasion. Potential push and pull forces at the tips of the invading cords were revealed by time-lapse imaging, which showed cells actively extending and retracting protrusions into the ECM. This 3D injury invasion model can be used to investigate mechanisms of leader cell–directed invasion and understand how mechanisms of wound healing are hijacked to cause disease.**

Monitoring Editor
Thomas M. Magin
University of Leipzig

Received: Sep 1, 2015
Revised: Dec 1, 2015
Accepted: Dec 2, 2015

INTRODUCTION

Invasiveness is a property typically associated with, but not exclusive to, cells that have acquired a cancer phenotype. The mechanisms regulating how groups of epithelial cells—normal or abnormal—are signaled to move collectively from their original site and invade a surrounding matrix environment are not completely understood. One important area for discovery concerns the origin and function of the cell types that direct such "collective invasion." Particularly relevant to this question are the many features shared between the processes of wound repair and cancer. The adage that tumors are "wounds that do not heal" (Dvorak, 1986; Kalluri and Zeisberg, 2006; Schafer and Werner, 2008) suggests that tumor progression hijacks mechanisms inherent to the wound-healing process. Both processes depend on similar soluble factors, including transforming growth factor β (Kalluri and Zeisberg, 2006; Rybinski *et al.*, 2014) and changes to their extracellular matrix environment (Rybinski *et al.*, 2014). In addition, there is strong correlation between genes that regulate wound healing and those central to cancer progression (Pedersen *et al.*, 2003; Chang *et al.*, 2004, 2005; Riss *et al.*, 2006). For example, 77% of genes induced for renal regeneration and repair are also up-regulated in renal cell carcinoma (Riss *et al.*, 2006). The gene expression profile of the cells located near the wound edge in skin wound healing is similar to that of squamous cell carcinoma cells (Pedersen *et al.*, 2003), and the "wound-response gene signature" of serum-activated fibroblasts in wound repair is also a strong clinical predictor of some of the deadliest forms of cancer (Chang *et al.*, 2004, 2005). Not surprisingly, then, the cell types that associate with an injured epithelium to modulate the repair process, such as macrophages and myofibroblasts, and those cells linked to fibrotic outcomes of wounding are also found in the tumor-associated stroma (Ronnov-Jessen *et al.*, 1996;

This article was published online ahead of print in MBoC in Press (http://www.molbiolcell.org/cgi/doi/10.1091/mbc.E15-09-0615) on December 10, 2015.

*Co–senior authors.

Address correspondence to: Janice L. Walker (janice.l.walker@jefferson.edu).

Abbreviations used: CMZ, central migration zone; OAZ, original attachment zone; SFM, serum-free medium.

Balkwill and Mantovani, 2001; Crowther *et al.*, 2001; Coussens and Werb, 2002; Leek and Harris, 2002; Kalluri and Zeisberg, 2006; Orimo and Weinberg, 2006; Schafer and Werner, 2008; Shimoda *et al.*, 2010). The similarities of the molecules/genes/cells involved in wound repair to those associated with the progression of metastatic cancers highlight the importance of studying whether cells that are activated upon wounding to direct the repair process have inherent invasive potential and the ability to direct a wounded epithelium to move through a matrix environment.

We addressed this question in studies of a clinically relevant wound model in which a mock cataract surgery is performed ex vivo and the resulting explant surrounded by Matrigel, thereby exposing the wounded tissue to a three-dimensional (3D) extracellular matrix environment typically used for cell invasion assays. Previously we showed that a subpopulation of vimentin-rich mesenchymal cells is activated in response to injury of the lens epithelium after mock cataract surgery. In that two-dimensional (2D) wound model, the activated mesenchymal cells migrate immediately to the wound edge, where they direct the collective migration of the injured epithelium across the cell-denuded endogenous basement membrane to close the wound (Walker *et al.*, 2010; Menko *et al.*, 2014). We showed that the function of the mesenchymal leader cells in the wound-repair process is dependent on the intermediate filament protein vimentin (Menko *et al.*, 2014). Also relevant to the present study, when these mesenchymal repair cells encounter a rigid microenvironment, they have a high potential to differentiate into myofibroblasts (Walker *et al.*, 2010). Mesenchymal cell–directed collective movement of the injured lens epithelium is highly reminiscent of the heterotypical stromal–epithelial cancer cell interactions that mediate collective invasion of tumor cells (Condeelis and Pollard, 2006; Gaggioli *et al.*, 2007; DeNardo *et al.*, 2009). Often, epithelial cancers break off from the primary tumor as strands or cords of cells, maintaining interactions with one another as they collectively invade, directed by leader cells (Khalil and Friedl, 2010; Friedl *et al.*, 2012; Clark and Vignjevic, 2015). The wound-repair process directed by the vimentin-rich cells of the lens provides an ideal reductionist model in which to investigate the role of mesenchymal cells in directing the collective invasion of epithelial cells through a 3D matrix. In our studies with this invasion-injury model, we found that many of the properties that give the mesenchymal cells of the lens the ability to direct wound repair also give them invasive potential. We anticipate that this ex vivo injury-invasion culture system will be a valuable model in which to investigate mechanisms by which leader cells direct invasion in multiple systems and be a pivotal step toward understanding how this process becomes hijacked to promote disease.

RESULTS

Injury-activated cells collectively invade 3D matrices

To study the invasive potential of cells activated in response to injury, we developed a 3D invasion assay in which ex vivo–wounded mock cataract surgery explants were placed cell side up on Matrigel-coated Transwells and then overlayed with a 3D Matrigel matrix. This approach created an environment in which the entire wounded explant was in direct contact with Matrigel (Figure 1A, model). Serum-containing medium was placed in the upper chamber on top of the Matrigel, and the bottom chamber was filled with serum-free medium (SFM), creating a modified chemoinvasion assay. This model for studying invasion was developed to mimic an in vivo matrix microenvironment. To follow whether cells activated upon wounding of the lens epithelium have invasive potential, we followed their behavior in the invasion assay using both a standard phase microscopy approach in which images were acquired daily (Figure 1, B and C) and time-lapse microscopy analysis (Figure 1, D and E; time lapse in Supplemental Video S1). As early as day 1 after wounding and being placed directly in the invasion assay, cells from the wounded cultures invaded into the Matrigel collectively as cords or strands of linked cells (Figure 1, B, arrow, and C, arrowhead; two separate regions shown at low power and high magnification, respectively). The appearance of the invaded cells was very similar to that previously reported for cords of tumor cells invading through a surrounding matrix (Friedl and Wolf, 2003; Friedl *et al.*, 2012; Clark and Vignjevic, 2015). With time, these invading cords of cells intersected with one another, eventually forming an anastomosed network within the Matrigel matrix (Figure 1, B and C). These invading cords were located throughout the 3D matrix, moving mostly through the area of this Matrigel matrix overlaying the lens capsule zone denuded of cells during the mock cataract surgery. Time-lapse imaging revealed the dynamic nature of the cells invading into Matrigel. As they invaded, the cells extended and retracted narrow protrusions into the 3D matrix environment (Supplemental Video S1 and Figure 1D). At the leading edge of the invading cords, the cells extended podosome-like processes (Supplemental Video S1 and Figure 1E) typical of invading cell types (Linder and Aepfelbacher, 2003). The cells from the wounded explant moved directly into the 3D ECM, traversing it as multicellular cords, and no cells were observed migrating across the denuded endogenous basement membrane of the lens as is typical of normal wound repair. As a result, in the 3D Matrigel environment, the wound left by the mock cataract surgery does not heal.

When grown in culture as 2D ex vivo explants after mock cataract surgery (as modeled in Figure 1A, left, top), the same cells heal the wounded area of the basement membrane quickly, with wound closure occurring within 3 d of the injury (Figure 2A; Menko *et al.*, 2014). Time-lapse imaging of 2D ex vivo wound-repair explants shows that the wounded lens epithelial cells moved collectively across the cell-denuded area of the endogenous lens basement membrane, with a leader-cell population at the wound edge (Figure 2B; time lapse in Supplemental Video S2). The leader cells in the 2D wound-repair cultures extended and retracted processes along the endogenous basement membrane of the wounded lens explant in the direction of movement (Figure 2B and Supplemental Video S2), similar to the behavior of leader cells invading through the 3D matrix environment (Figure 1, D and E, and Supplemental Video S1). Although these properties of the leader cells are shared in the wound-repair and wound-invasion models, the behavior of the epithelial follower cells is distinct. In the 2D environment, the epithelial cells move across the basement membrane as a sheet. The epithelial cells maintain cell–cell contacts, their lateral organization as an intact epithelial monolayer, and their association with the basement membrane capsule of the lens (Figure 2, A and B). In contrast, as these epithelial cells follow the leader cells into and through the 3D Matrigel matrix, they reorganize into cords of cells, and although they remain linked to one another, they lose their adhesion to their endogenous basement membrane (Figure 1, B and C). These results show that although the normal wound-healing response of an injured epithelium is regeneration of the tissue structure, when the cells that typically lead the wound-repair process encounter an altered matrix microenvironment, they have significant invasive potential that influences the migratory behavior of their associated epithelium.

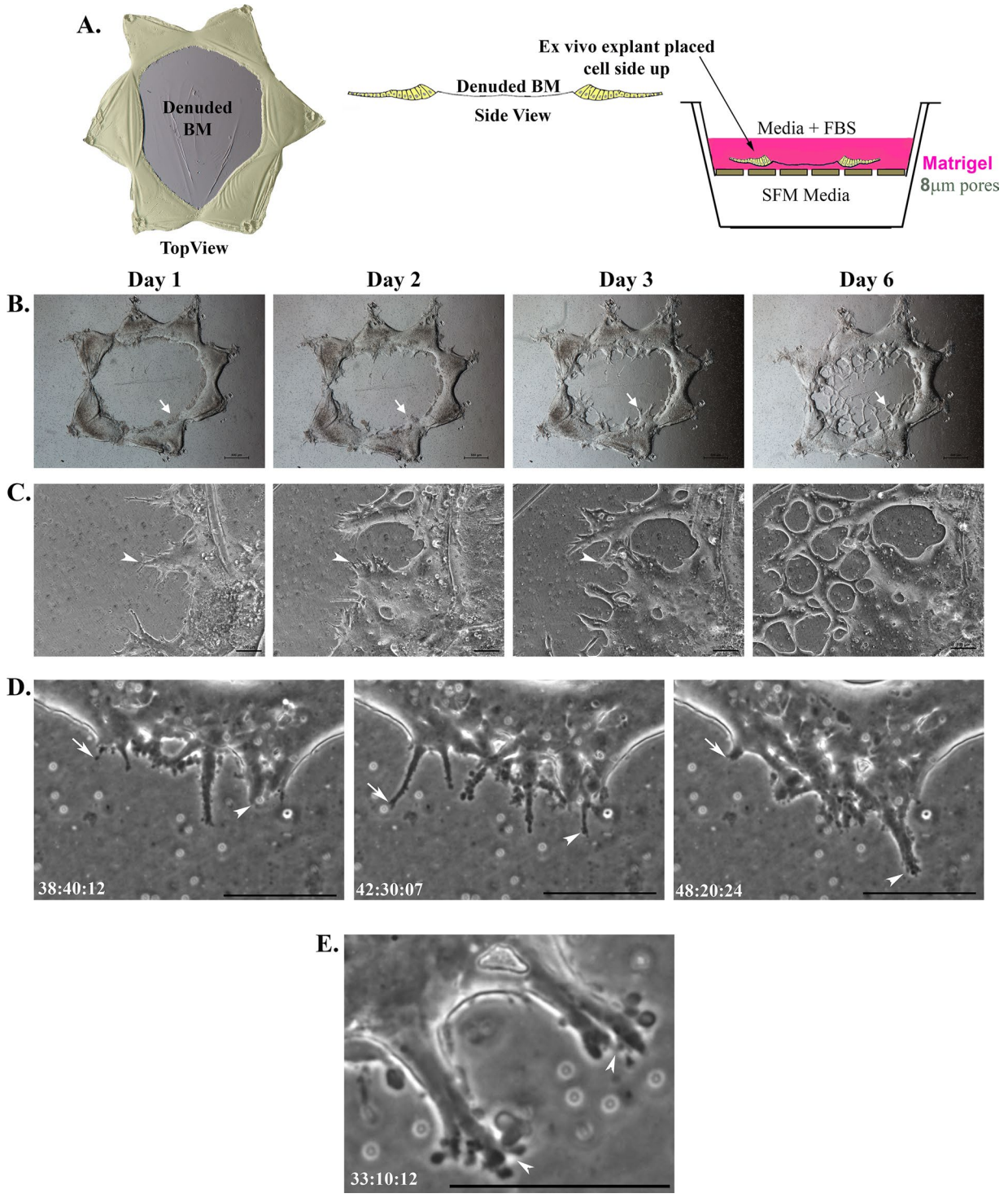

FIGURE 1: Cells invade collectively as cords in 3D invasion assays in response to injury. (A) Model depicting the ex vivo injury explant 3D invasion assay. Diagrams are shown of the ex vivo explants after cataract surgery (injury) as both top and side views. The lens epithelial cells remaining associated with the lens basement membrane (BM) after injury that results from removal of the lens fiber cell mass are shaded in yellow. For the 3D invasion assays, these ex vivo injury explants were placed cell side up on top of Matrigel-coated Transwell filters and overlayed with Matrigel. The top chamber is filled with serum-containing medium and the lower chamber with SFM. (B, C) Phase contrast images documenting invasion of cells from the ex vivo–injured culture explants from days 1–6. By day 1, cells began to invade as cords of cells into the Matrigel matrix above the explant (B, low magnification, arrow; C, high magnification, arrowhead). Cells continued to invade into Matrigel as cords and intersected to form an anastomizing cell network (C; day 3, arrowhead). Bars, 500 μm (B), 100 μm (C). (D) Still images from time-lapse microscopy revealed cells at the tip of the invading cord dynamically extending (arrowhead) and retracting (arrow) within the 3D matrix. Bar, 10 μM. (E) Still image at high magnification from time-lapse microscopy (Supplemental Video S1), showing podosome-like processes formed at tips of cells leading the invading cords (arrowheads). Bar, 10 μM. In D and E, time is presented as hours:minutes:seconds.

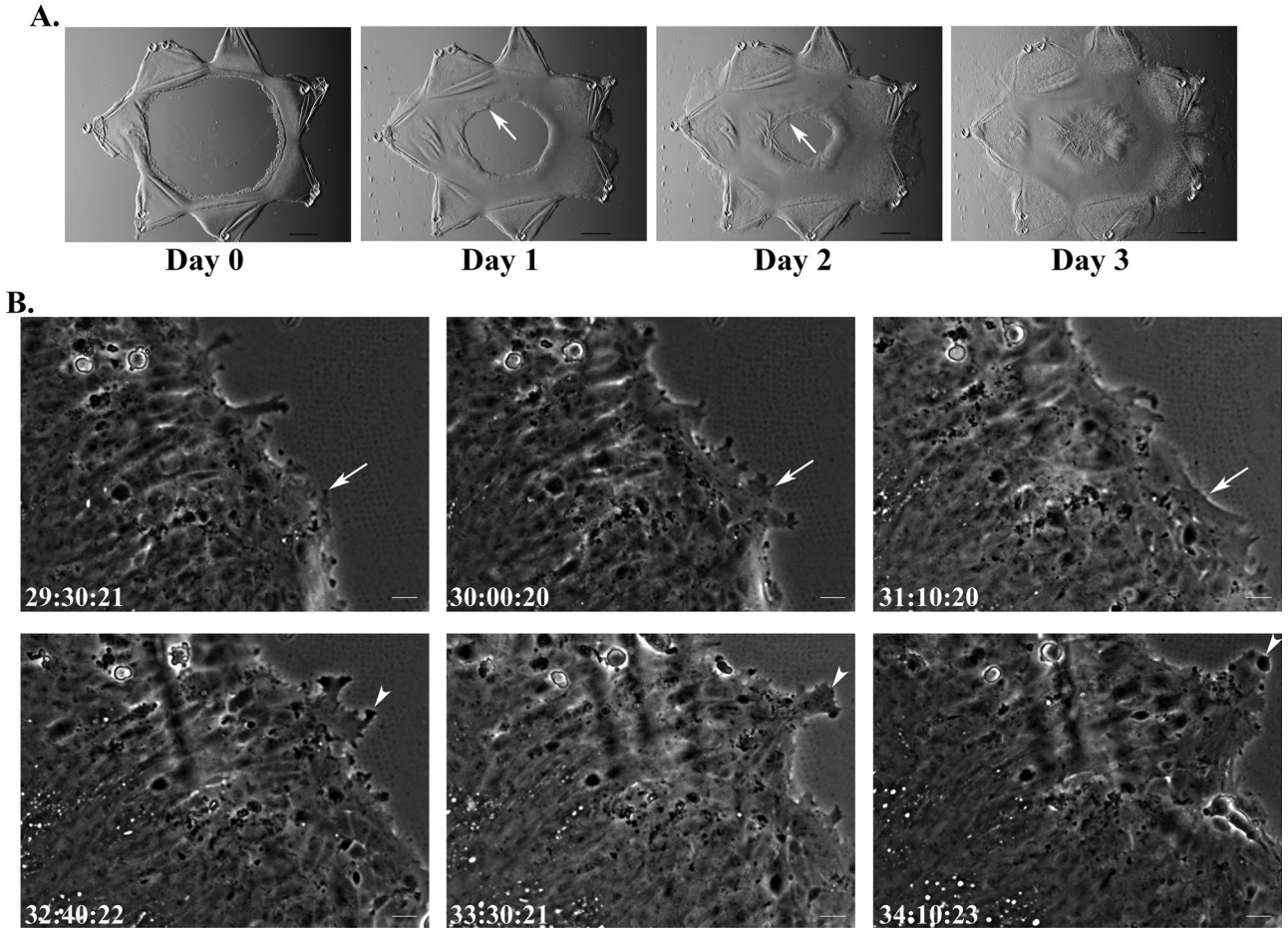

FIGURE 2: Cells migrate collectively as a sheet in response to injury in 2D ex vivo wound-repair explants. (A) Phase contrast images documenting wound healing in the ex vivo wound-repair explants from days 0–3. In response to injury, in the 2D model, cells move together as a collective sheet onto the denuded basement membrane to close the wound (arrow). By day 3, wound healing is typically completed. Bar, 500 μm. (B) Still images from time-lapse microscopy (Supplemental Video S2), demonstrating the collective movement of cells as they respond to injury to heal the wound. At the wound edge, leader cells extend and retract protrusions (arrowhead, arrow) along the basement membrane in a dynamic manner as wound healing proceeds. Epithelial cells behind the leading edge maintain cell–cell contact with one another, as well as their association with the endogenous lens basement membrane capsule, as they collectively heal the wound. Bar, 20 μm. In B, time is presented as hours:minutes:seconds.

Mesenchymal cells that direct lens wound repair have functional properties consistent with their ability to invade through a matrix microenvironment when activated in response to injury

In the 2D wound-repair model, the mesenchymal cell subpopulation directs the collective movement of the wounded lens epithelium from their original attachment zone (OAZ) along the equatorial aspects of the lens basement membrane capsule across the central migration zone (CMZ) to heal the wound. The CMZ is the area on the posterior lens capsule denuded of cells when the lens fiber cell mass is removed during the microsurgical procedure (modeled in Figure 3A). Our previous investigations of this 2D ex vivo mock cataract surgery wound model showed that a mesenchymal subpopulation of the lens is activated immediately upon injury to migrate to the wound edge of the injured epithelium and that this leader-cell population is rich in the intermediate filament protein vimentin. We discovered that vimentin function is essential to the ability of these mesenchymal cells to direct the collective movement of the injured lens epithelium to repair the wound (Menko *et al.*, 2014). Given that the leader cells in the 3D Matrigel wound-invasion model we now study behave similarly to the mesenchymal cells at the leading edge of the 2D mock cataract surgery wound-repair model, we examined whether the vimentin-rich repair cells in the 2D wound-healing model express molecules that could endow them with invasive properties. The molecules associated with invasion competence we investigated included the hyaluronic cell adhesion receptor CD44, known to be critical to both the migratory and invasive behavior of many cell types (Lopez *et al.*, 2005; Misra *et al.*, 2015; Thomas *et al.*, 1992), and the matrix metalloproteinases (MMPs) MMP-9 (gelatinase B) and MMP-2 (gelatinase A), which enable cell invasion by degrading the extracellular matrix (Pulkoski-Gross, 2015). Western blot analysis for these molecules was performed on the cells in the active zone of migration (CMZ) of the ex vivo wound repair explants and those in the OAZ after their separation by microdissection. These studies were performed from 1 to 3 d after injury, with day 3 the time when wound healing was completed. The results showed that CD44, MMP-9, and MMP-2 were predominately expressed in the CMZ (Figure 3, B–D), with a prevalence in this zone of the active

enzymatic forms of both MMP-2 and MMP-9 (Figure 3, C and D, bottom arrows). Expression of CD44, MMP-9, and MMP-2 was highest at D1 after wounding and decreased significantly as wound healing was completed (Figure 3, B–D).

Immunofluorescence analysis was performed on the 2D wounded lens explants at day 1 postinjury to determine whether induction of CD44, MMP-9, and/or MMP-2 in the CMZ observed in the biochemical analysis reflected the specific expression of these molecules by the vimentin-rich mesenchymal repair cells that had located to the wound edge. For these studies, the wounded explants were immunolabeled for vimentin and colabeled for CD44 (Figure 3, E–G), MMP-9 (Figure 3, H–J), or MMP-2 (Figure 3, K–M). CD44 was localized to the cell borders of the vimentin-rich leader cells at the wound edge and was also concentrated at the tips of protrusions extended by these cells along the denuded basement membrane (Figure 3, E–G, arrow). The vimentin$^+$ cells at the wound edge also expressed MMP-2 and MMP-9, the latter of which had a distinctive punctate staining pattern that extended into the cellular processes. This pattern of localization included MMP-9–rich puncta along the protrusions elaborated by the vimentin-rich leader cells (Figure 3, H–J, arrow), as well as MMP-9–rich puncta that extended beyond the leading edge of the cells onto the endogenous basement membrane capsule on which the cells will migrate (Figure 3, H–J, arrowhead). This staining pattern likely reflects MMP-9 in its secreted form and its involvement in clearing the path along the matrix substrate of any cellular material that remained after injury. There was a strong colocalization of MMP-9 with vimentin intermediate filaments of these cells (Figure 3, H–J), which extended to the tips of the mesenchymal repair cells at the wound edge (arrow), suggesting a coordinate role for these molecules. Of interest, inhibiting the function of MMP-2 and/or MMP-9 slightly slowed but did not prevent wound closure (Figure 3N), indicating that whereas MMPs may facilitate effective wound repair, their function was not essential to promote the movement of the epithelium to repair the wound. Nonetheless, these results demonstrated that the mesenchymal leader cells involved in wound repair produce proteases that are key to their ability to invade when encountering an altered matrix environment.

Vimentin-rich mesenchymal cells of the lens activated to direct wound repair have intrinsic invasive potential

As an alternative approach to the 3D Matrigel invasion assay, we also used the classical Matrigel-Transwell invasion assay to examine the invasive potential of cells activated upon lens epithelial wounding after mock cataract surgery. For these studies, ex vivo–wounded mock cataract surgery explants were placed cell side down on the Matrigel-coated, cell-permeable membrane of the Transwell. SFM was placed in the upper chamber and serum-containing medium in the lower chamber to create a chemoinvasion assay (Figure 4A, model). Cells able to invade through the Matrigel coating on the Transwell filter gain access to pores through which they can migrate to the underside of the filter membrane. After 3 d, cells were scraped from the top of the filter, and any cells that had invaded to the bottom of the Transwell filter were detected by labeling with the histological stain Diff Quick and imaged by microscopy (Figure 4B). This analysis revealed that small groups of cells from the wounded explants were competent to invade through the Matrigel and the Transwell filter to the underside of the membrane, confirming that after a mock cataract surgery, a population of cells from the wounded lens had acquired invasive potential.

We examined whether properties associated with the function of the vimentin$^+$ mesenchymal cells in directing repair of the lens epithelium in two dimensions impart to these same cells their potential to invade in three dimensions and lead the collective invasion of their associated epithelium. For these studies, the wounded mock cataract surgery lens explants were plated cell side down in the Matrigel-Transwell invasion assay. Immunolocalization studies were performed to determine whether, like the mesenchymal cells at the leading edge of the wounded epithelium, the cells that had invaded through the Matrigel-coated Transwell to reach the underside of the Transwell filter coexpress vimentin and CD44. Image analysis demonstrated that invaded cells were vimentin$^+$/CD44$^+$, identifying them as activated repair cells (Figure 5, A–C). In the 2D mock cataract surgery cultures, the mesenchymal subpopulation activated to mediate the repair process highly express vimentin, whereas filamentous (F)-actin labels both the mesenchymal leader cells and the follower cells of the lens epithelium (Menko *et al.*, 2014; Walker *et al.*, 2010). To examine whether the ability to migrate to the filter bottom in the Matrigel-Transwell assay was a specific property of the vimentin$^+$ repair cell population, the invaded cells were labeled for both vimentin and F-actin at day 2 of the assay. Quantification of 30 invaded colonies from eight wounded explants for the percentage of F-actin$^+$ cells expressing vimentin showed that 100% of the total invaded cells (F-actin$^+$) were mesenchymal leader cells (vimentin$^+$). A defining characteristic of invading cells is the presence of invadopodia and podosomes, cellular structures collectively referred to as invadosomes (Linder, 2009). These actin-rich structures enable invading cells to both degrade and adhere to an extracellular matrix environment, making it possible for them to migrate through the ECM (Linder, 2007; Linder *et al.*, 2011; Saltel *et al.*, 2011; Destaing *et al.*, 2014). To further support our discovery that the vimentin-rich repair cells have invasive properties, we immunolabeled the cells that had invaded to the bottom of the Matrigel-Transwell filter for key signature molecules of invadosomes, including the scaffold protein Tks5 (Courtneidge *et al.*, 2005; Blouw *et al.*, 2008; Di Martino *et al.*, 2014), the actin-cytoskeletal regulator cortactin (Bowden *et al.*, 1999; Artym *et al.*, 2006, 2008; Clark *et al.*, 2007), and matrix metalloproteinases. Image analysis showed that the invaded cells were rich in the invadopodia molecules cortactin, Tks5, MMP-2, and MMP-9 (Figure 5, D–L). Coimmunolabeling for cortactin with Tks5, MMP-2 with MMP-9, and cortactin with MMP-9 showed many regions of the invaded cells in which these molecules that impart invasion competence were codistributed.

Coimmunostaining for vimentin and F-actin was also performed without scraping the cells from the top of the filter membrane in order to be able to visualize cells in the process of invading through the Matrigel-coated Transwell membrane in the Transwell invasion assay. Consecutive optical sections were collected from the top of the inverted ex vivo explant that is sitting on the Matrigel-coated Transwell filter (which corresponds to the bottom of the lens capsule) through to the bottom of the Transwell filter by confocal imaging. In Figure 5M, a single optical plane is shown of a vimentin-rich mesenchymal cell that has invaded through to the bottom of the filter. Imaris image analysis software was used to create a 3D view of the same cell on the filter from the collected confocal *z*-stack, which showed the invaded vimentin-rich repair cell identified in Figure 5M moving through a Transwell filter pore to the underside of the filter (Figure 5N). These results demonstrate that the mesenchymal cells activated upon injury to regulate the wound-repair process have acquired properties that classify them as invasive in a classical invasion assay.

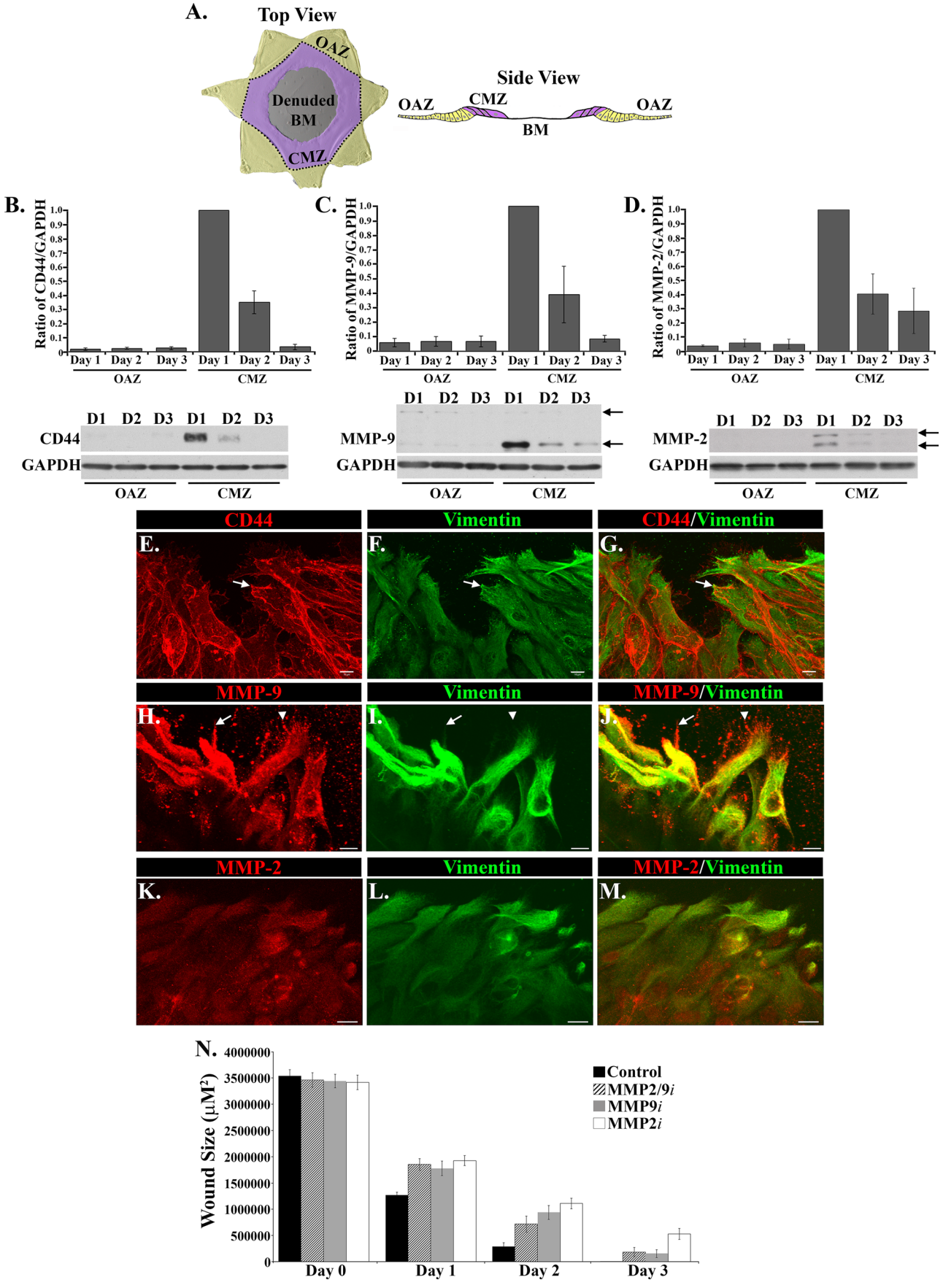
A.
Top View
OAZ
Denuded BM
CMZ
Side View
OAZ
CMZ
OAZ
BM
B.
Ratio of CD44/GAPDH
C.
Ratio of MMP-9/GAPDH
D.
Ratio of MMP-2/GAPDH
Day 1
Day 2
Day 3
OAZ
CMZ
D1 D2 D3 D1 D2 D3
CD44
GAPDH
MMP-9
MMP-2
CD44
Vimentin
CD44/Vimentin
MMP-9
MMP-9/Vimentin
MMP-2
MMP-2/Vimentin
E.
F.
G.
H.
I.
J.
K.
L.
M.
N.
Wound Size (μM²)
4000000
3500000
3000000
2500000
2000000
1500000
1000000
500000
0
Control
MMP2/9i
MMP9i
MMP2i
Day 0
Day 1
Day 2
Day 3

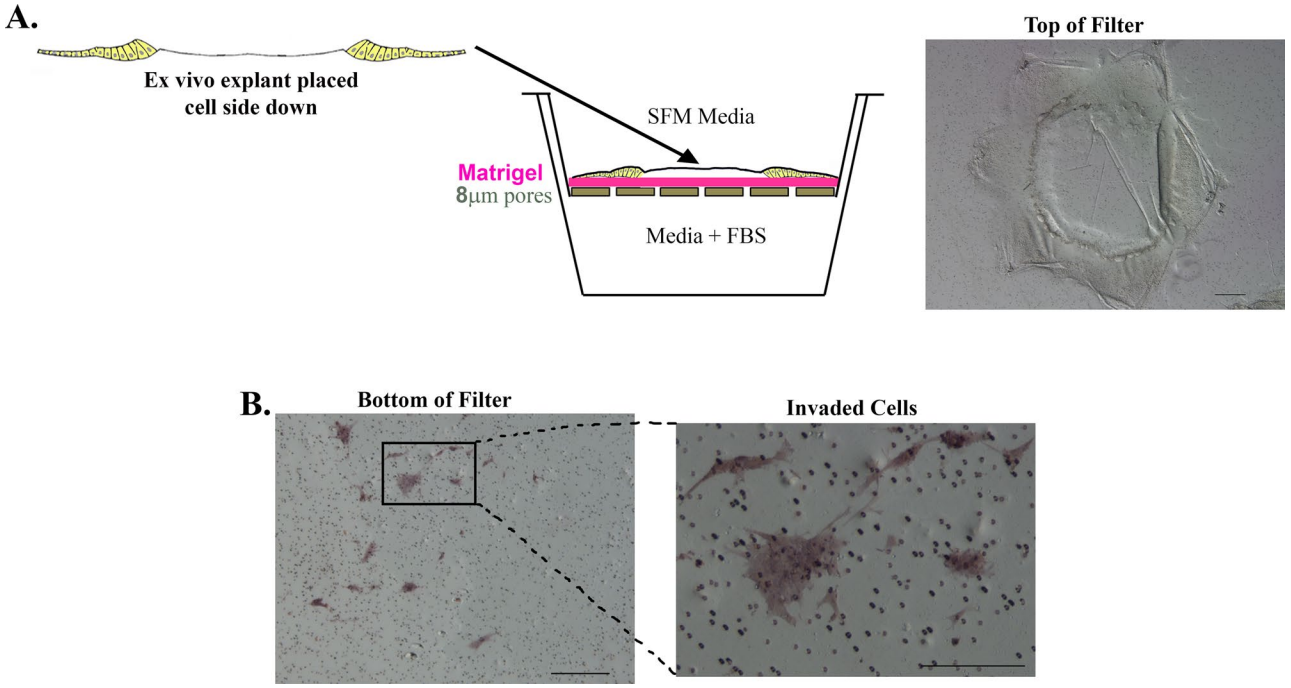

FIGURE 4: In response to injury, a subpopulation of cells becomes competent to invade in a classic Matrigel invasion assay. (A) Model depicting Matrigel-Transwell invasion assay with ex vivo injury explants. For these studies, explants were placed cell side down on Matrigel-coated Transwell filters. The top chamber was filled with SFM medium and the lower chamber with complete medium containing fetal bovine serum to create a chemoinvasion assay. Right, a phase contrast image of the ex vivo explant placed cell side down on top of the Matrigel filter. (B) After 3 d in culture, the explants on top of the filter were removed by scraping, and the cells that had invaded and migrated to the bottom of the filters were labeled with the histological stain Diff Quick. Right, invaded cells at higher magnification. Bar, 200 μm.

Mesenchymal cells that direct epithelial tissue repair also can promote invasion of the wounded epithelium

Together our previous findings that vimentin-rich mesenchymal cells are activated upon wounding of an epithelium to direct the collective movement of the injured epithelium to close the wound and our discovery here that these same mesenchymal cells have significant invasive potential suggest that these activated mesenchymal cells could also signal the collective invasion of their associated wounded epithelium. To examine this question, we immunolabeled cells from wounded mock cataract surgery explants that had invaded in the 3D

FIGURE 3: Mesenchymal leader cells in the 2D ex vivo injury culture model are enriched for molecules involved in invasion, CD44, MMP-2, and MMP-9. (A) Model of the different regions of the ex vivo mock cataract surgery explant that are separated by microdissection for this study from both top and side views. Cells found in the points of the star-shaped culture that contain the region of the lens that is occupied by epithelial cells in vivo are referred to as the original attachment zone (OAZ, yellow). In response to injury, cells move onto the denuded basement membrane (BM) into the central migration zone (CMZ, purple). (B–D) To examine whether there are migration-specific changes in expression of molecules associated with invasion after wounding, ex vivo injury explants were microdissected into OAZ and CMZ regions and extracted on days 1–3 for Western blot analysis for CD44, MMP-9, MMP-2, and GAPDH (loading control). Graphs depicting Western blot results from four independent studies show the relative expression of CD44, MMP-9, and MMP-2 to GAPDH. CD44, MMP-9, and MMP-2 were predominately expressed in the CMZ region. These molecules decreased in expression as wound healing progressed on day 2 and on day 3, when wound healing is typically completed. MMP-2 and MMP-9 were detected predominantly in their active forms (bottom arrows) compared with their inactive proenzymatic form (top arrows). For both MMP-2 and MMP-9, the active form (lower band) was quantified and is represented on the graphs as a ratio to GAPDH. Immunoblots were quantified using Kodak 1D software, and data were normalized to results at day 1 in the CMZ zone. Values for each graph and relative densities are plotted ±SEM. Representative Western blots are shown below each graph. (E–M) Ex vivo–wounded cultures were fixed and immunostained for vimentin (F, I, L; green) and colabeled for CD44 (E, G; red), MMP-9 (H, J; red), or MMP-2 (K, M; red). Vimentin-rich mesenchymal cells at the leading edge were enriched for MMP-2, MMP-9, and CD44. CD44 localized at cell–cell interfaces and to the tips of these cells at the leading edge (E–G, arrow). MMP-9 strongly localized to vimentin-rich cells, sometimes colocalized with vimentin (H–J, arrow) and also to regions in the area to be repaired just beyond the cells (H, J, arrowhead). Bar, 10 μm. (N) The role of MMP-2/9 function on wound healing in the 2D ex vivo injury cultures was evaluated using inhibitors to MMP-2, MMP-9, or MMP-2/9. Phase images were taken on days 0–3, from which the open wound area was calculated in at least six capsules and quantified using NIS Elements analysis software. Open wound area was plotted on the graphs ±SEM. Inhibition of MMP-2 and/or MMP-9 function resulted in only a slight delay in wound closure.

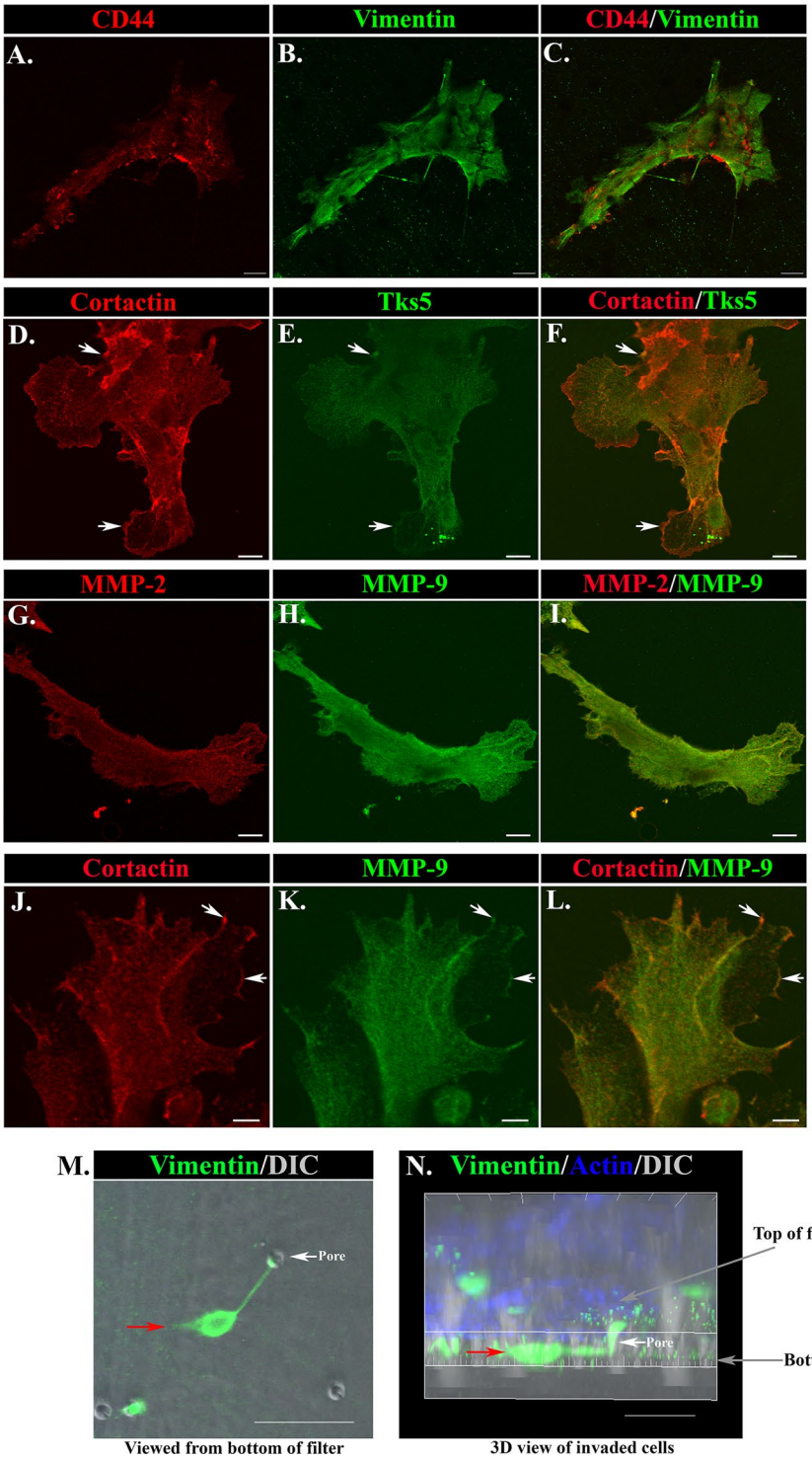

FIGURE 5: CD44/vimentin-rich mesenchymal cells that express markers of invadosomes are inherently invasive in Matrigel-Transwell chemoinvasion assays. (A–C) At 2 d in culture, cells that have invaded to the bottom of Matrigel-coated Transwell filters were coimmunostained for vimentin and CD44. Identification of these invaded cells as mesenchymal was determined by their positive labeling for both CD44 (A, C; red) and vimentin (B, C; green). Bar, 20 μM. (D–L) Cells that invaded in the Matrigel-Transwell chemoinvasion assays were labeled for characteristic invadosome molecules on day 2. Invaded cells were coimmunostained for the following combinations: cortactin (D, F; red) with Tks5 (E, F; green); MMP-2 (G, I; red) with MMP-9 (H, I; green); or cortactin (J, L; red) with MMP-9 (K, L; green). Invaded cells were rich in all invadopodia molecules examined, and regions of colabeling for cortactin and Tks5 (D–F, arrows), as well as cortactin and MMP-9 (J–L, arrows) were evident where these molecules may function in invadosomes for invasive function. Bar = 10 μm (D–I), 5 μm (J–L). (M, N) A Matrigel-Transwell chemoinvasion assay at 24 h in culture labeled for vimentin (green) and F-actin (blue) and also imaged by differential interference contrast (DIC). (M) A single vimentin-rich mesenchymal cell that had invaded through Matrigel to the bottom of the filter through a pore in the filter (seen as a hole in the DIC image; white arrow) is imaged en face, represented by the red arrow. Bar, 50 μm. (N) The same cell (red arrow) as shown in a 3D reconstruction side view of confocal *Z*-stacks collected from the explant basement membrane capsule of the inverted explant on top of the filter through to the cells that had invaded to the bottom of the filter. Here the transit of this cell through the filter pore (white arrow) is evident. Bar, 30 μM. Here A–C and M–N are Matrigel-Transwell chemoinvasion assays in which the explant on top of the filter was not removed before immunostaining. In D–L, the explant on top of the filter was removed before labeling.

Matrigel invasion assay over 6 d with antibody to vimentin and colabeled them with fluorescent-conjugated phalloidin to detect F-actin. Vimentin staining will highlight the vimentin-rich mesenchymal repair cells that had migrated into the Matrigel matrix, and F-actin will label all cells that had invaded into Matrigel, including lens epithelial cells. Images of cells were collected at many consecutive optical planes throughout the Matrigel matrix by confocal microscopy and 3D reconstructions prepared from the collected *z*-stacks with Imaris software (Figure 6). These 3D images are presented as both top-down (Figure 6A) and side (Figure 6B) views. Both vimentin-rich mesenchymal cells (vimentin-rich/F-actin$^+$) and epithelial cells (vimentin-poor/F-actin$^+$) had invaded the Matrigel matrix, led by the mesenchymal cells.

An orthogonal view of the same confocal *z*-stack shows that the vimentin-rich repair cells are located at the front of the invading cord that is moving upward through the Matrigel, followed by a collective group of actin-rich, vimentin-poor follower cells (Figure 6C). To demonstrate the epithelial phenotype of the invading "follower" cells being led through the Matrigel by the vimentin-rich mesenchymal repair cell population, we colabeled the cells that had invaded the Matrigel from the wounded explants for vimentin and the tight junction molecule ZO-1, which is enriched in epithelial cells. The cords of cells invading the Matrigel matrix were led by the vimentin-rich mesenchymal cells and followed into the 3D matrix by a collective group of ZO-1–rich epithelial cells (Figure 6, D and E). From

these studies, we conclude that the mesenchymal cells activated to modulate the normal repair process of a wounded lens epithelium can also signal the collective invasion of normal epithelial cell populations in response to injury. The 3D invasion ex vivo injury culture system is a powerful model in which to investigate heterotypical mesenchymal–epithelial cell interactions involved in regulating collective invasion.

Functional properties of wound repair–activated cell invasion

Vimentin has been linked to functional roles in cell migration and invasion. It is highly expressed in the cells at the leading edge of the cords of injured lens tissue that invade through the Matrigel 3D matrix (Figure 7A) and extends into the invadosomes that these cells project into the surrounding matrix. Whereas formation of invadopodia is an actin-dependent event, their further growth and elongation is dependent on intermediate filament networks (Schoumacher *et al.*, 2010). Also typical of invadopodia structures, the processes extended by the vimentin-rich mesenchymal cells also label strongly for cortactin (Figure 7, B and C) and alpha–smooth muscle actin (αSMA; Figure 7, E and G). αSMA localized primarily in puncta that extended into the tips of the invading cells (Figure 7, E–G). Little F-actin was detected in regions enriched for αSMA puncta (Figure 7, E and G; arrowhead), suggesting that αSMA is organized in a globular form that may exert specific mechanical forces in regulating the invasion of these cells. Invadopodia function in degrading/remodeling the matrix environment to enable the cells to invade. Consistent with this finding, the vimentin-rich mesenchymal cells leading the cords of injured lens cells through the 3D Matrigel matrix express high levels of MMP-9, which appears to be secreted in vesicular structures that often extend just beyond the tips of these leading edge cells into the surrounding matrix environment (Figure 7D). To investigate the function of MMP-2, MMP-9, and vimentin in invasion of wound-activated cells, we performed the Matrigel-Transwell invasion assay in the presence of inhibitors of each of these molecules. Invasion was suppressed in the Matrigel-Transwell assay by functionally inhibiting vimentin, MMP-2, MMP-9, or a combination of MMP-2 and MMP-9 (Figure 7H). The MMP2/9 inhibitor II reduced invasion by 84% (Figure 7H), the MMP-2 inhibitor II by 99%, and the MMP-9 inhibitor I by 96%. Vimentin function was inhibited with withaferin A (WFA), which blocked invasion by 98% (Figure 7H). Whereas WFA can have some off-target affects, previous studies by our lab and others show that its effects on cell migration properties match that of vimentin knockdowns (Menko *et al.*, 2014). These studies suggest essential roles for both matrix metalloproteinases and the intermediate filament protein vimentin in promoting cell invasion in response to injury.

DISCUSSION

Understanding the mechanisms that induce groups of cells to become migratory and collectively invade their surrounding microenvironment remains an ongoing challenge. An essential step toward elucidating the mechanisms that drive collective invasion is identifying the origin and function of the cells that act as the directors/leaders of this process. Our results revealed that the vimentin-rich mesenchymal cells activated upon wounding of epithelial tissues to direct the repair process have invasive potential and the ability to direct a normal wounded epithelium through a 3D matrix environment. We investigated the invasive behavior of such cells in response to injury by placing tissue explants from a physiologically relevant ex vivo wound-repair model in a 3D matrix environment. Vimentin-rich mesenchymal cells were observed at the leading tips of invading cords of cells, followed through the 3D matrix by a ZO-1–positive epithelial cell population. We propose that this 3D injury/invasion model is a valuable system in which to elucidate mechanisms regulating collective invasion in response to injury, such as the functional properties of leader cells and the role of heterotypical leader–follower cell interactions in this process. To our knowledge, this is the first demonstration that a cell type linked to the regulation of wound repair can direct the collective invasion of normal epithelium when activated in response to injury. Given the similar properties shared between wound healing and cancer progression, findings with this model have the potential to positively affect our understanding of how mechanisms of wound repair, such as collective invasion, can be hijacked for disease progression.

Heterotypical interactions between leader and follower cells appear fundamental for the collective invasion of a cohort of cells. Our results suggest that a "normal" epithelium, without mutation, can acquire invasive ability in response to injury due to the heterotypic interactions with mesenchymal leader cells. In this case, leader and follower cells can enter into a mutually beneficial relationship, one that allows the epithelial cells to retain their epithelial characteristics while using the migratory and invasive properties of the leader cells to drive the collective invasion of the group of cells. Because normal epithelial cells are typically not inherently invasive, we hypothesize that the mesenchymal leader cells are generating a path through the ECM for the epithelial cells to follow. In support of this hypothesis, a number of studies demonstrate that leader cells can generate paths or tracks through both proteolytic and structural (force-mediated) mechanisms to remodel the matrix environment to promote collective invasion of follower cells (Friedl and Wolf, 2003; Gaggioli *et al.*, 2007; Gaggioli, 2008; Radisky, 2007; Wolf *et al.*, 2007; Olson, 2010; Scott *et al.*, 2010; Crighton and Olson, 2011). In the present study, we found that MMP-2/9 proteolytic function was necessary for collective invasion in response to injury. MMP-9 was enriched in the leader-cell population at the tips of cords of invading cells and found in vesicular-like structures outside the cell borders, where it could function to proteolytically degrade and remodel the matrix to create a path for collective invasion. Time-lapse imaging revealed the dynamic behavior of the cells at the leading edge of the cords, showing that they actively extend and retract cellular protrusions. This property is likely to reflect dynamic "push" and "pull" forces that are present at the leading invasive front of the cord of cells essential to promote the forward movement of the group of cells through the 3D ECM. Consistent with this hypothesis, a recent study demonstrated that dynamic tensile forces drive the movement of cohorts of cells through 3D ECM (Gjorevski *et al.*, 2015). In that study, tensile mechanosensitive forces are increased at the invasive front, allowing the cells to grip and pull on the matrix for movement through the 3D environment (Gjorevski *et al.*, 2015). Instead of exerting continuous tensile force on the microenvironment, the cells exhibit periods of extension and retraction (Gjorevski *et al.*, 2015). We propose that the leader cells at the tips of the invading cord of cells in our injury/invasion model participate in MMP-mediated matrix remodeling and creating dynamic tensile (push and pull) forces necessary to create a path for collective invasion.

Vimentin has long been recognized as a major regulator of invasion; however, how vimentin functions to mediate this process is not yet clear. Increased vimentin expression is often associated with cell invasion (Thompson *et al.*, 1992; Schaafsma *et al.*, 1993; Dushku and Reid, 1994; Gilles *et al.*, 1996), and its loss can inhibit invasion in a number of different cancer cell types (Singh *et al.*, 2003; Wei *et al.*, 2008). Vimentin was a prominent feature of the cells at the leading front of the invading cords in our injury/invasion model, where they extended vimentin-rich protrusions

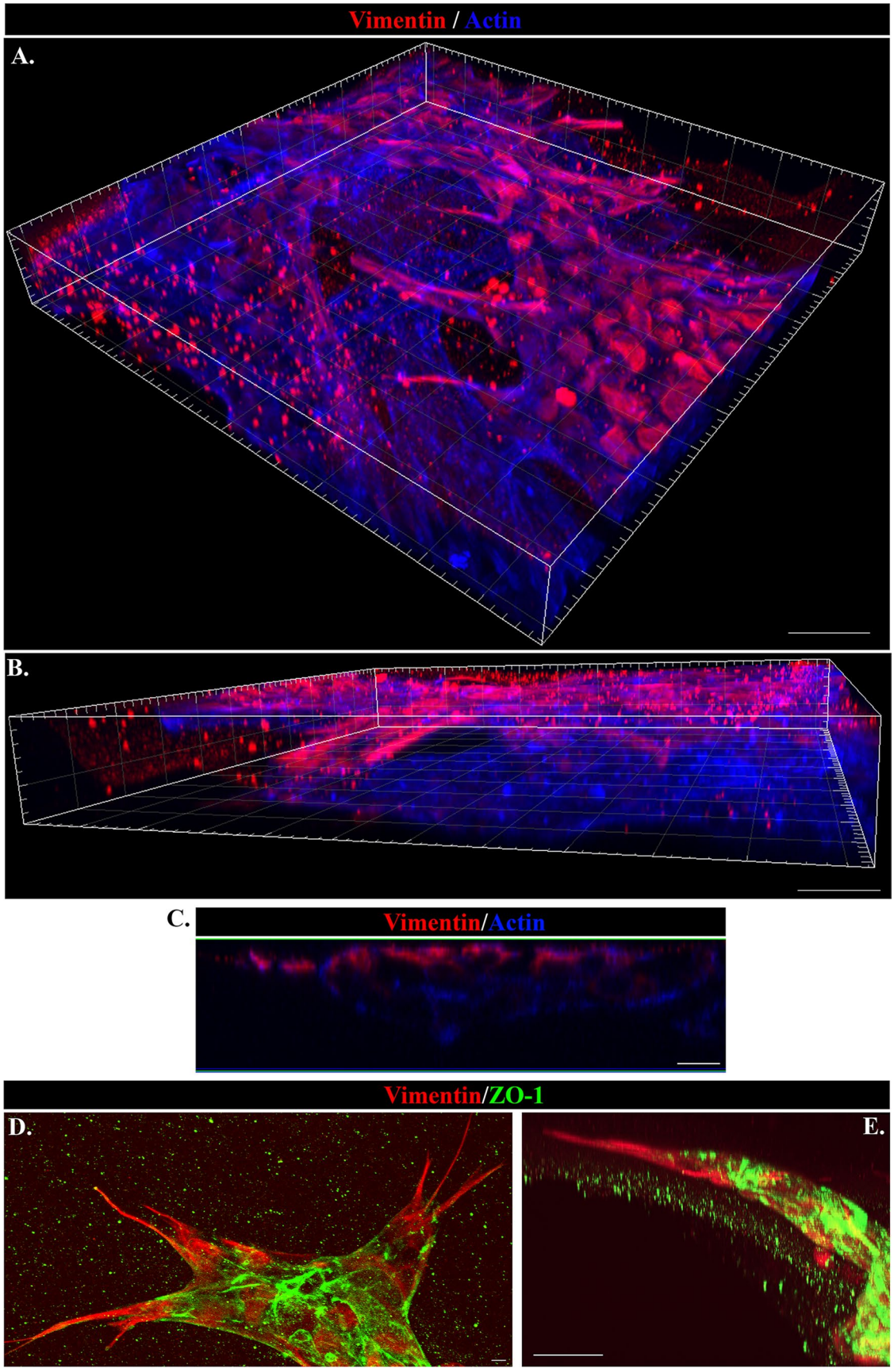

FIGURE 6: Vimentin-rich mesenchymal cells are the leader cells in collective invasion of the wounded lens epithelium through 3D Matrigel. (A–E) The 3D Matrigel invasion assay of ex vivo–wounded explants at day 6 in culture. (A, B) Imaris 3D reconstruction from confocal *Z*-stacks of cords of cells that have invaded into the Matrigel matrix labeled for

into the Matrigel. We found that treatment with WFA, which inhibits vimentin function, prevented collective invasion of the wounded epithelium, suggesting a key role for vimentin in regulating collective invasion in response to injury. We propose that vimentin intermediate filaments are necessary for the cells at the tips of invading cords to extend and stabilize protrusions for invasion into the 3D matrix environment. In support of this hypothesis, vimentin intermediate filaments are reported to regulate the elongation and stabilization of invadopodia (Schoumacher *et al.*, 2010; Sutoh Yoneyama *et al.*, 2014), which our studies show are a prominent feature of the invading mesenchymal leader cells. Because vimentin intermediate filaments (IFs) are well known for their tensile strength, this cytoskeletal element is a likely candidate for participating in the dynamic force generation (push and pull forces) at the tips of the cords of cells that is needed to drive invasion. Changes in vimentin organization between assembly into an IF network and disassembly could regulate the dynamic extension and retraction behavior that we observe at the front edge of invasion in our injury invasion assay. Phosphorylation is one major mechanism by which vimentin organization could be dynamically regulated at the tips of the invading cells (Izawa and Inagaki, 2006; Ivaska *et al.*, 2007; Sihag *et al.*, 2007; Snider and Omary, 2014). Protrusion formation and force generation at the tips of invading cells likely involve the coordinated action of both the actin and vimentin intermediate filament cytoskeleton. We found that the tips of the invading vimentin-rich cells were enriched for the invadopodia molecules cortactin and Tks5 and the contractile actin protein αSMA. Strikingly, αSMA was primarily detected in puncta in regions with low-level staining for F-actin. This result suggests that αSMA is present in a globular form in regions at the tips of invading cords that are also rich in vimentin. Given that αSMA organized into stress fibers is associated with contractile function, different assembly states of αSMA may impart distinct functional properties. We propose that αSMA in a punctate distribution may contribute to mechanical forces at the invading edge. Together vimentin and αSMA may coordinate mechanical forces at the tips of invading cords involved in regulating the dynamic pushing and pulling forces for collective invasion.

Study of the invasive function of vimentin-rich leader cells, a cell type that functions to regulate injury repair, and their ability to direct the wounded epithelium through the 3D matrix may provide insight into the mechanisms of wound repair that are associated with cancer cell progression. The 3D injury invasion model provides a valuable system in which to investigate the process of collective invasion involving heterotypical leader–follower cell function. This model can be used to identify therapeutic targets and test strategies to modulate the collective invasion process with application to treating and preventing disease progression.

MATERIALS AND METHODS

Ex vivo epithelial injury model preparation and imaging

To prepare ex vivo epithelial injury explants, lenses were removed from embryonic day 15 (E15) chicken (B&E Eggs) eyes by dissection (Walker *et al.*, 2007, 2010) and prepared as described (Walker *et al.*, 2015). An incision was made in the anterior lens capsule, the thick basement membrane that surrounds the lens. Lens fiber cell mass was removed by hydroelution (Walker *et al.*, 2007, 2010, 2015). Five cuts were made in the anterior region of this tissue, creating additional wound edges that allowed the explants to be flattened and pinned to the culture dish cell side up (Figure 1A). Cells in the 3D invasion and 2D wound-healing models were followed by microscopic imaging using Nikon Eclipse Ti-S (Nikon, Tokyo, Japan) or AZ100 (Nikon) microscopes and imaging software (NIS Elements; Nikon). To follow the behavior of invading cells in three dimensions and wound healing in two dimensions, time-lapse imaging was performed using a Tokai Hit stage-top incubator on a Nikon Eclipse TE2000-U microscope or Nikon Eclipse Ti microscope driven by image analysis software (NIS Elements). The ex vivo epithelial explants were cultured in Media 199 (Invitrogen, Carlsbad, CA) containing 1% penicillin/streptomycin (Mediatech-Cellgro, Manassas, VA) and 1% L-glutamine (Mediatech-Cellgro) with or without 10% fetal calf serum (Invitrogen, Carlsbad, CA) as specified. To inhibit MMP-2 and/or MMP-9 function, ex vivo explants were grown in the presence of inhibitors to MMP-2 (20 μM; Millipore, Billerica, MA), MMP-9 (20 μM; Millipore), or MMP-2/9 (25 μM; Millipore). To perturb vimentin function, ex vivo explants were grown in the presence of WFA (1.5 μM; Tocris, Ellisville, MO). Inhibitors were dissolved in dimethyl sulfoxide and added to the culture medium. In all inhibitor experiments, control cultures were incubated in the presence of vehicle. Fresh inhibitor was added each day.

Western blot analysis

Samples were extracted and lysed in TX/OG buffer (44.4 mM *n*-octyl β-D-glucopyranoside, 1% Triton X-100, 100 mM NaCl, 1 mM $MgCl_2$, 5 mM EDTA, 10 mM imidazole) containing 1 mM sodium vanadate, 0.2 mM H_2O_2, and a protease inhibitor cocktail (Sigma-Aldrich, St. Louis, MO). Protein concentrations were determined with the bicinchoninic acid assay (Pierce, Rockford, IL). Proteins were separated on Tris-glycine gels (Novex, San Diego, CA), electrophoretically transferred to membrane (Immobilon-P; Millipore, Billerica, MA), and immunoblotted as described previously (Walker and Menko, 1999). For detection, ECL reagent (Amersham Life Sciences, Arlington Heights, IL) was used. Immunoblots were scanned, and densitometry analysis was performed (1D software; Eastman Kodak, Rochester, NY). The ratio of each protein to glyceraldehyde 3-phosphate dehydrogenase (GAPDH) was calculated for each sample and normalized to the ratio at day 1 in the CMZ and graphed ±SEM. Gels for CD44 analysis were run under nonreducing conditions; gels

vimentin (red) and F-actin (blue), viewed from (A) top down and (B) the side. Vimentin-rich cells are directing the invasion of the cords of F-actin–rich cells upward through the Matrigel, as evidenced by their location to the leading edges of the cords. Bar, 30 μm. (C) An orthogonal cut of the same confocal *Z*-stack of invading cords of cells shown as a 3D reconstruction in A and B demonstrates from another angle that the vimentin-rich mesenchymal cells (red) had invaded into the Matrigel in the leader position as directors of associated wounded epithelial cells (blue). Bar, 10 μm. (D, E) Invading cords of cells in the 3D Matrigel invasion assay immunolabeled for vimentin (red) and the epithelial cell–cell adhesion protein ZO-1 (green) and imaged by confocal microscopy. The image in D is a projection of a *Z*-stack and illustrates that the vimentin-rich cells are located at the leader position of invading cords of ZO-1–rich epithelial cells. Bar, 5 μm. One area of the cords shown in D is viewed in E as a 3D reconstruction, viewed from the side, which emphasizes the leader position of the vimentin-rich mesenchymal cells (red) relative to a follower cord of epithelial cells (ZO-1; green). Bar, 30 μm.

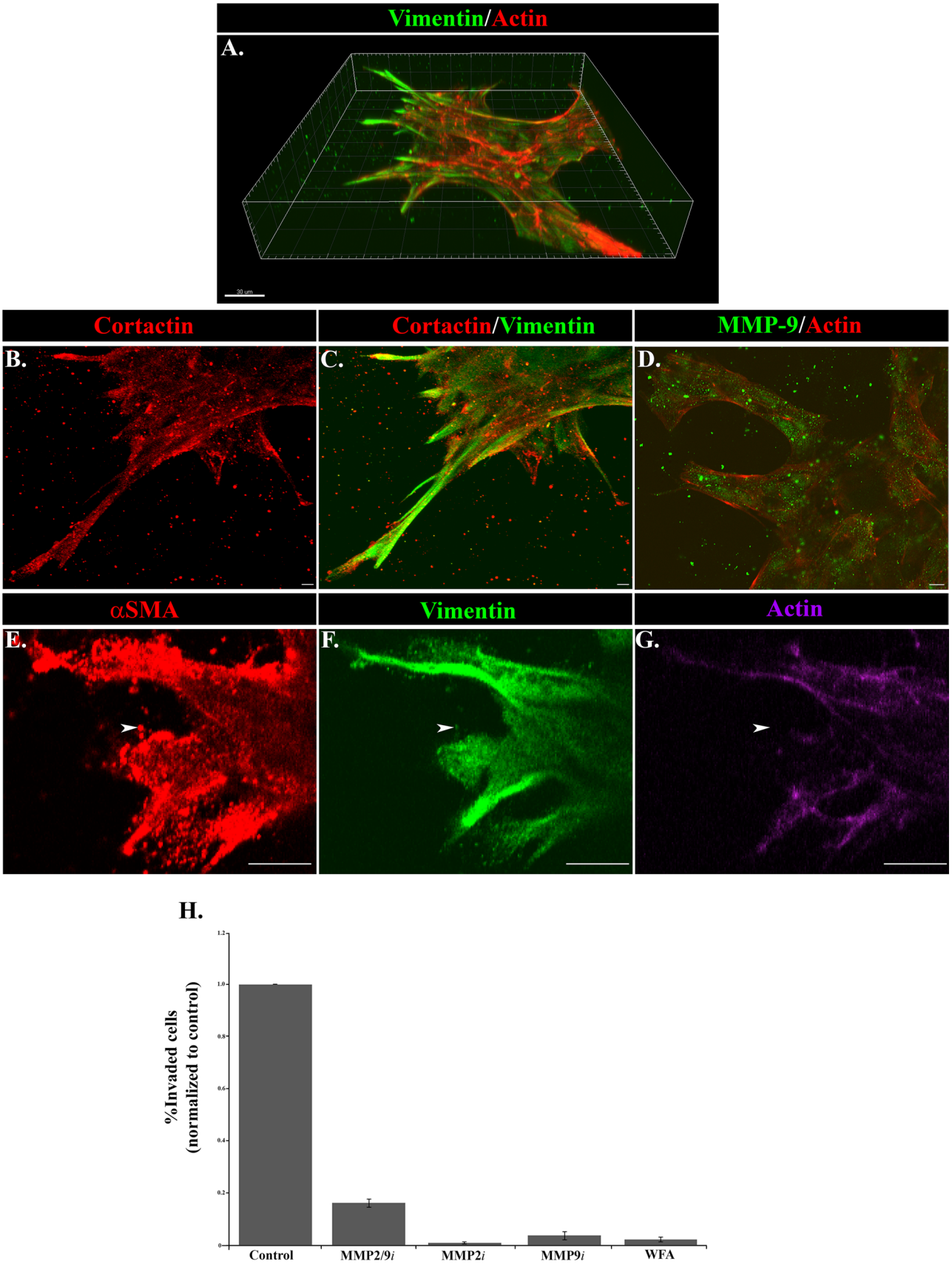

FIGURE 7: Functional properties of invading cells in response to injury. (A–G) The 3D Matrigel invasion assay of ex vivo–wounded explants at (A–D) day 6 in culture and (E–G) day 2 in culture. (A) A 3D reconstruction of a confocal *Z*-stack of cords of cells in the injury invasion assay labeled for vimentin (green) and F-actin (red), emphasizing the extension of vimentin-rich cells into the Matrigel matrix in leader-cell positions. Bar, 30 μm. (B, C) Cords of invading cells

in the Matrigel invasion assay were immunolabeled for cortactin (red) and vimentin (green) and viewed by confocal microscopy. This projection image of a confocal *Z*-stack shows that the processes extended by the vimentin-rich mesenchymal cells into the Matrigel also expressed cortactin (red). Bar, 5 µm. (D) Labeling for MMP-9 (green) in cells at the leading edges of the cords extended into Matrigel and was distributed in discrete vesicular structures in the cells (F-actin; red) and also in a punctate pattern just beyond the cells in the Matrigel matrix, where it can act to degrade the matrix for invasion. A representative single optical plane captured by confocal microscopy. Bar, 10 µm. (E–G) Vimentin-rich cells at the invading front (green) also express αSMA (red), often with a punctate distribution (arrowhead). Labeling for F-actin (purple) was mostly absent from the areas with a strong distribution of αSMA puncta, suggesting that this actin population was nonfilamentous. A representative single optical plane captured by confocal microscopy. Bar, 10 µm. (H) The individual roles of MMP-2/9 and vimentin in invasion after wounding were evaluated using an inhibitor approach in the Matrigel-Transwell chemoinvasion assay. This study included the MMP-2 inhibitor MMP-2*i*, the MMP-9 inhibitor MMP-9*i*, the combined MMP-2/9 inhibitor MMP-2/9*i*, and the vimentin inhibitor WFA. Invaded cells from at least 10 capsules were counted and quantified using MetaMorph or NIS Elements image analysis software. Relative numbers of invaded cells were plotted on graphs ±SEM. MMP-2 and MMP-9 function were required for invasion of cells in the Matrigel-Transwell assay. MMP-2 inhibited invasion by 99%, MMP-9 by 96%, and MMP2/9 by 84% in the Matrigel-Transwell assays. Inhibiting vimentin function with WFA suppressed invasion in the Matrigel-Transwell assay by 98%.

for MMP-9 and MMP-2 analysis were run under reducing conditions. Antibodies used for Western blotting included CD44 (monoclonal antibody [mAb]; Developmental Studies Hybridoma Bank, Iowa City, IA), MMP-9 (polyclonal; Millipore), MMP-2 (monoclonal; Millipore), and GAPDH (Santa Cruz Biotechnology, Santa Cruz, CA).

Immunofluorescence

Wounded explants were immunostained as described previously (Walker *et al.*, 2007, 2010). Explants were fixed in 3.7% formaldehyde in phosphate-buffered saline (PBS) and permeabilized in 0.25% Triton X-100 (Sigma-Aldrich) in PBS before immunostaining. For 3D invasion studies, explants were fixed in 4% paraformaldehyde in PBS and permeabilized in 0.5% Triton X-100. Cells were incubated with primary antiserum, followed by rhodamine- or Alexa Fluor 488–conjugated secondary antibodies (Jackson ImmunoResearch Laboratories, West Grove, PA). Primary antibodies used for the immunofluorescence studies included vimentin (mAb; Developmental Studies Hybridoma Bank), MMP-9 (polyclonal; Millipore), MMP-2 (mAb; Millipore), cortactin (Millipore), Tks5 (polyclonal; Millipore) and, αSMA (Sigma-Aldrich). The vimentin polyclonal antibody was a generous gift from Paul FitzGerald (University of California, Davis, Davis, CA) Some explants were counterstained with Alexa Fluor 488– or 633–conjugated phalloidin (Invitrogen-Molecular Probes, Carlsbad, CA), which binds F-actin. Immunostained samples were examined by confocal microscopy (LSM 510; Zeiss, Thornwood, NY). Either single images or *Z*-stacks were collected and analyzed. Data are presented as single optical planes, projection images, or orthogonal sections imaged from the apical to basal direction. The 3D images of confocal *Z*-stacks were created with Imaris software (BitPlane, Concord, MA).

Invasion assays

To assay invasion, explants resulting from a mock cataract surgery were placed in either a Matrigel-Transwell invasion assay or a 3D Matrigel invasion assay. For the Matrigel-Transwell assays, ex vivo–wounded explants were placed cell side down onto the Matrigel-coated membrane (BD Biosciences, San Jose, CA; and Corning, Corning, NY). For this assay, SFM was placed in the upper chamber and serum-containing medium in the lower chamber to create a chemoinvasion assay. The underside of the membrane containing invaded cells was either stained for histological analysis with Diff quick (IMEB, San Marcos, CA) or analyzed by immunofluorescence staining. For inhibitor studies, ex vivo explants were preincubated with inhibitor before placement in the Matrigel-Transwell assays, with fresh inhibitor added each day. To calculate the number of cells that invaded in the Transwell assay, the underside (invaded side) of the filters was stained with 4′,6-diamidino-2-phenylindole (Invitrogen, Grand Island, NY) and total nuclei counted in a region corresponding to the area where the explant had been placed in the top chamber. The average number of cells treated with vehicle or inhibitor for each experiment was calculated and normalized to vehicle control. The average normalized values are represented graphically. For 3D Matrigel invasion assays, ex vivo–wounded explants were placed cell side up in Matrigel Transwells and overlayed with 3 mg/ml Matrigel (BD Biosciences and Corning). For these studies, serum-containing medium was placed in the upper chamber and SFM in the lower chamber. Cultures were imaged live by phase and time-lapse microscopy or fixed and immunostained for proteins of interest.

ACKNOWLEDGMENTS

We thank Liping Zhang for excellent technical assistance and Paul Fitzgerald (University of California, Davis, School of Medicine, Davis, CA) for providing us with the vimentin polyclonal antibody. The monoclonal antibodies AMF17b (vimentin; developed by Alice B. Fulton, University of Iowa Carver College of Medicine, Iowa City, IA) and 1D10 (CD44; developed by Willi Halfter, University of Pittsburgh, Pittsburgh, PA) were obtained from the Developmental Studies Hybridoma Bank, created by the National Institute of Child Health and Human Development of the National Institutes of Health and maintained at the Department of Biology, University of Iowa (Iowa City, IA). This work was supported by National Institutes of Health Grant EY021784 to A.S.M. and Grant IRG-08-060-01 from the American Cancer Society to J.L.W.

REFERENCES

Artym VV, Zhang Y, Seillier-Moiseiwitsch F, Yamada KM, Mueller SC (2006). Dynamic interactions of cortactin and membrane type 1 matrix metalloproteinase at invadopodia: defining the stages of invadopodia formation and function. Cancer Res 66, 3034–3043.

Ayala I, Baldassarre M, Giacchetti G, Caldieri G, Tete S, Luini A, Buccione R (2008). Multiple regulatory inputs converge on cortactin to control invadopodia biogenesis and extracellular matrix degradation. J Cell Sci 121, 369–378.

Balkwill F, Mantovani A (2001). Inflammation and cancer: back to Virchow? Lancet 357, 539–545.

Blouw B, Seals DF, Pass I, Diaz B, Courtneidge SA (2008). A role for the podosome/invadopodia scaffold protein Tks5 in tumor growth in vivo. Eur J Cell Biol 87, 555–567.

Bowden ET, Barth M, Thomas D, Glazer RI, Mueller SC (1999). An invasion-related complex of cortactin, paxillin and PKCmu associates with invadopodia at sites of extracellular matrix degradation. Oncogene 18, 4440–4449.
Chang HY, Nuyten DS, Sneddon JB, Hastie T, Tibshirani R, Sorlie T, Dai H, He YD, van't Veer LJ, Bartelink H, *et al.* (2005). Robustness, scalability, and integration of a wound-response gene expression signature in predicting breast cancer survival. Proc Natl Acad Sci USA 102, 3738–3743.
Chang HY, Sneddon JB, Alizadeh AA, Sood R, West RB, Montgomery K, Chi JT, van de Rijn M, Botstein D, Brown PO (2004). Gene expression signature of fibroblast serum response predicts human cancer progression: similarities between tumors and wounds. PLoS Biol 2, E7.
Clark AG, Vignjevic DM (2015). Modes of cancer cell invasion and the role of the microenvironment. Curr Opin Cell Biol 36, 13–22.
Clark ES, Whigham AS, Yarbrough WG, Weaver AM (2007). Cortactin is an essential regulator of matrix metalloproteinase secretion and extracellular matrix degradation in invadopodia. Cancer Res 67, 4227–4235.
Condeelis J, Pollard JW (2006). Macrophages: obligate partners for tumor cell migration, invasion, and metastasis. Cell 124, 263–266.
Courtneidge SA, Azucena EF, Pass I, Seals DF, Tesfay L (2005). The SRC substrate Tks5, podosomes (invadopodia), and cancer cell invasion. Cold Spring Harb Symp Quant Biol 70, 167–171.
Coussens LM, Werb Z (2002). Inflammation and cancer. Nature 420, 860–867.
Crighton D, Olson MF (2011). Trailblazing LIM kinases take the lead in collective tumor cell invasion. Bioarchitecture 1, 5–8.
Crowther M, Brown NJ, Bishop ET, Lewis CE (2001). Microenvironmental influence on macrophage regulation of angiogenesis in wounds and malignant tumors. J Leukoc Biol 70, 478–490.
DeNardo DG, Barreto JB, Andreu P, Vasquez L, Tawfik D, Kolhatkar N, Coussens LM (2009). CD4(+) T cells regulate pulmonary metastasis of mammary carcinomas by enhancing protumor properties of macrophages. Cancer Cell 16, 91–102.
Destaing O, Petropoulos C, Albiges-Rizo C (2014). Coupling between actoadhesive machinery and ECM degradation in invadosomes. Cell Adh Migr 8, 256–262.
Di Martino J, Paysan L, Gest C, Lagree V, Juin A, Saltel F, Moreau V (2014). Cdc42 and Tks5: a minimal and universal molecular signature for functional invadosomes. Cell Adh Migr 8, 280–292.
Dushku N, Reid TW (1994). Immunohistochemical evidence that human pterygia originate from an invasion of vimentin-expressing altered limbal epithelial basal cells. Curr Eye Res 13, 473–481.
Dvorak HF (1986). Tumors: wounds that do not heal. Similarities between tumor stroma generation and wound healing. N Engl J Med 315, 1650–1659.
Friedl P, Locker J, Sahai E, Segall JE (2012). Classifying collective cancer cell invasion. Nat Cell Biol 14, 777–783.
Friedl P, Wolf K (2003). Tumour-cell invasion and migration: diversity and escape mechanisms. Nat Rev Cancer 3, 362–374.
Gaggioli C (2008). Collective invasion of carcinoma cells: when the fibroblasts take the lead. Cell Adh Migr 2, 45–47.
Gaggioli C, Hooper S, Hidalgo-Carcedo C, Grosse R, Marshall JF, Harrington K, Sahai E (2007). Fibroblast-led collective invasion of carcinoma cells with differing roles for RhoGTPases in leading and following cells. Nat Cell Biol 9, 1392–1400.
Gilles C, Polette M, Piette J, Delvigne AC, Thompson EW, Foidart JM, Birembaut P (1996). Vimentin expression in cervical carcinomas: association with invasive and migratory potential. J Pathol 180, 175–180.
Gjorevski N, A SP, Varner VD, Nelson CM (2015). Dynamic tensile forces drive collective cell migration through three-dimensional extracellular matrices. Sci Rep 5, 11458.
Ivaska J, Pallari HM, Nevo J, Eriksson JE (2007). Novel functions of vimentin in cell adhesion, migration, and signaling. Exp Cell Res 313, 2050–2062.
Izawa I, Inagaki M (2006). Regulatory mechanisms and functions of intermediate filaments: a study using site- and phosphorylation state-specific antibodies. Cancer Sci 97, 167–174.
Kalluri R, Zeisberg M (2006). Fibroblasts in cancer. Nat Rev Cancer 6, 392–401.
Khalil AA, Friedl P (2010). Determinants of leader cells in collective cell migration. Integr Biol (Camb) 2, 568–574.
Leek RD, Harris AL (2002). Tumor-associated macrophages in breast cancer. J Mammary Gland Biol Neoplasia 7, 177–189.
Linder S (2007). The matrix corroded: podosomes and invadopodia in extracellular matrix degradation. Trends Cell Biol 17, 107–117.
Linder S (2009). Invadosomes at a glance. J Cell Sci 122, 3009–3013.
Linder S, Aepfelbacher M (2003). Podosomes: adhesion hot-spots of invasive cells. Trends Cell Biol 13, 376–385.
Linder S, Wiesner C, Himmel M (2011). Degrading devices: invadosomes in proteolytic cell invasion. Annu Rev Cell Dev Biol 27, 185–211.
Lopez JI, Camenisch TD, Stevens MV, Sands BJ, McDonald J, Schroeder JA (2005). CD44 attenuates metastatic invasion during breast cancer progression. Cancer Res 65, 6755–6763.
Menko AS, Bleaken BM, Libowitz AA, Zhang L, Stepp MA, Walker JL (2014). A central role for vimentin in regulating repair function during healing of the lens epithelium. Mol Biol Cell 25, 776–790.
Misra S, Hascall VC, Markwald RR, Ghatak S (2015). Interactions between hyaluronan and its receptors (CD44, RHAMM) regulate the activities of inflammation and cancer. Front Immunol 6, 201.
Olson MF (2010). Follow the leader: LIM kinases pave the way for collective tumor cell invasion. Cell Cycle 9, 4417–4418.
Orimo A, Weinberg RA (2006). Stromal fibroblasts in cancer: a novel tumor-promoting cell type. Cell Cycle 5, 1597–1601.
Pedersen TX, Leethanakul C, Patel V, Mitola D, Lund LR, Dano K, Johnsen M, Gutkind JS, Bugge TH (2003). Laser capture microdissection-based in vivo genomic profiling of wound keratinocytes identifies similarities and differences to squamous cell carcinoma. Oncogene 22, 3964–3976.
Pulkoski-Gross AE (2015). Historical perspective of matrix metalloproteases. Front Biosci (School Ed) 7, 125–149.
Radisky DC (2007). Leading the charge. Nat Cell Biol 9, 1341–1342.
Riss J, Khanna C, Koo S, Chandramouli GV, Yang HH, Hu Y, Kleiner DE, Rosenwald A, Schaefer CF, Ben-Sasson SA, *et al.* (2006). Cancers as wounds that do not heal: differences and similarities between renal regeneration/repair and renal cell carcinoma. Cancer Res 66, 7216–7224.
Ronnov-Jessen L, Petersen OW, Bissell MJ (1996). Cellular changes involved in conversion of normal to malignant breast: importance of the stromal reaction. Physiol Rev 76, 69–125.
Rybinski B, Franco-Barraza J, Cukierman E (2014). The wound healing, chronic fibrosis, and cancer progression triad. Physiol Genomics 46, 223–244.
Saltel F, Daubon T, Juin A, Ganuza IE, Veillat V, Genot E (2011). Invadosomes: intriguing structures with promise. Eur J Cell Biol 90, 100–107.
Schaafsma HE, Van Der Velden LA, Manni JJ, Peters H, Link M, Rutter DJ, Ramaekers FC (1993). Increased expression of cytokeratins 8, 18 and vimentin in the invasion front of mucosal squamous cell carcinoma. J Pathol 170, 77–86.
Schafer M, Werner S (2008). Cancer as an overhealing wound: an old hypothesis revisited. Nat Rev Mol Cell Biol 9, 628–638.
Schoumacher M, Goldman RD, Louvard D, Vignjevic DM (2010). Actin, microtubules, and vimentin intermediate filaments cooperate for elongation of invadopodia. J Cell Biol 189, 541–556.
Scott RW, Hooper S, Crighton D, Li A, Konig I, Munro J, Trivier E, Wickman G, Morin P, Croft DR, *et al.* (2010). LIM kinases are required for invasive path generation by tumor and tumor-associated stromal cells. J Cell Biol 191, 169–185.
Shimoda M, Mellody KT, Orimo A (2010). Carcinoma-associated fibroblasts are a rate-limiting determinant for tumour progression. Semin Cell Dev Biol 21, 19–25.
Sihag RK, Inagaki M, Yamaguchi T, Shea TB, Pant HC (2007). Role of phosphorylation on the structural dynamics and function of types III and IV intermediate filaments. Exp Cell Res 313, 2098–2109.
Singh S, Sadacharan S, Su S, Belldegrun A, Persad S, Singh G (2003). Overexpression of vimentin: role in the invasive phenotype in an androgen-independent model of prostate cancer. Cancer Res 63, 2306–2311.
Snider NT, Omary MB (2014). Post-translational modifications of intermediate filament proteins: mechanisms and functions. Nat Rev Mol Cell Biol 15, 163–177.
Sutoh Yoneyama M, Hatakeyama S, Habuchi T, Inoue T, Nakamura T, Funyu T, Wiche G, Ohyama C, Tsuboi S (2014). Vimentin intermediate filament and plectin provide a scaffold for invadopodia, facilitating cancer cell invasion and extravasation for metastasis. Eur J Cell Biol 93, 157–169.
Thomas L, Byers HR, Vink J, Stamenkovic I (1992). CD44H regulates tumor cell migration on hyaluronate-coated substrate. J Cell Biol 118, 971–977.
Thompson EW, Paik S, Brunner N, Sommers CL, Zugmaier G, Clarke R, Shima TB, Torri J, Donahue S, Lippman ME, *et al.* (1992). Association of increased basement membrane invasiveness with absence of estrogen receptor and expression of vimentin in human breast cancer cell lines. J Cell Physiol 150, 534–544.

Walker JL, Bleaken BM, Wolff IM, Menko AS (2015). Establishment of a clinically relevant ex vivo mock cataract surgery model for investigating epithelial wound repair in a native microenvironment. J Vis Exp 2015, e52886.
Walker JL, Menko AS (1999). alpha6 Integrin is regulated with lens cell differentiation by linkage to the cytoskeleton and isoform switching. Dev Biol 210, 497–511.
Walker JL, Wolff IM, Zhang L, Menko AS (2007). Activation of SRC kinases signals induction of posterior capsule opacification. Invest Ophthalmol Visual Sci 48, 2214–2223.
Walker JL, Zhai N, Zhang L, Bleaken BM, Wolff I, Gerhart J, George-Weinstein M, Menko AS (2010). Unique precursors for the mesenchymal cells involved in injury response and fibrosis. Proc Natl Acad Sci USA 107, 13730–13735.
Wei J, Xu G, Wu M, Zhang Y, Li Q, Liu P, Zhu T, Song A, Zhao L, Han Z, *et al*. (2008). Overexpression of vimentin contributes to prostate cancer invasion and metastasis via src regulation. Anticancer Res 28, 327–334.
Wolf K, Wu YI, Liu Y, Geiger J, Tam E, Overall C, Stack MS, Friedl P (2007). Multi-step pericellular proteolysis controls the transition from individual to collective cancer cell invasion. Nat Cell Biol 9, 893–904.